JOURNAL OF APPLIED POLYMER SCIENCE VOL. 16, PP. 2777–2794 (1972)

Characterization of Poly(methyl Methacrylate) from Radiation-Induced Polymerization in the Presence of a Kaolin Clay Substrate

J. J. BEESON and K. G. MAYHAN, *Department of Chemical Engineering and Graduate Center for Materials Research, University of Missouri-Rolla, Rolla, Missouri 65401*

Synopsis

Two types of polymer are formed in the radiation-initiated polymerization of methyl methacrylate (MMA)–kaolin clay complexes. Homopolymer can be extracted from the complex by the use of organic solvents. Inserted polymer must be removed by dissolution of the polymer–clay complex with hydrofluoric acid. The polymers formed show no differences in structure (as determined by infrared analysis), had high molecular weights (1–5 $\times$ 10^6), and had similar molecular weight distributions (as determined by GPC). The molecular weights of the homopolymer increased as temperature increased (25°–75°C), and dose rate decreased (24.9–7.35 rads/sec). The isotacticity of the polymers when compared to irradiated bulk polymer decreased as follows: inserted > homo > bulk. The compressive properties of the irradiated composite compared well with those of commercial bulk polymers. Degradation temperatures were 20° to 30°C higher for the composite than for the commercial chemically initiated bulk polymer.

INTRODUCTION

Since 1960, different authors have done polymer characterization work on various types of composite systems. These systems included MMA and styrene in the presence of metal and inorganic oxides.[1,2]

In a series of papers, Blumstein and co-workers have characterized the methyl acrylate (MA)-, MMA-, and MMA-crosslinked systems polymerized in the presence of sodium montmorillonites. They were especially interested in the polymer grafted to the clay, which was called "inserted polymer." In Blumstein's first paper[3] on the preparation of the inserted polymer, both free-radical catalysts (benzoyl peroxide, azobisisobutyronitrile) and gamma rays (0.4 Mrads/hr) were used as initiators. Blumstein stated that the bulk monomer was almost entirely polymerized at an intensity of 0.1 Mrad, while the composite needed much higher doses. Composites which initially contained up to 25% MMA polymerized, and only inserted polymer was recovered. Composites containing higher initial percentages of MMA polymerized and contained both inserted and homopolymer (polymer which can be recovered by extraction with normal solvents). No spontaneous polymerization occurred in the system. The thermal degradation at 215°C of the complex showed that the inserted

polymer resisted degradation even when the conventional bulk polymer was totally destroyed.[4] This fact was attributed to the steric structure of the clay which restricted the thermal motion of the polymer. Oxygen greatly accelerated the degradation process. Blumstein and Billmeyer[5] studied the dilute solution properties of the three systems and found that the poly(methyl acrylate) (PMA) and crosslinked insertion PMMA systems had quite different properties from the conventional bulk polymer. The differences included high light-scattering molecular weights combined with low viscosities, low second virial coefficients, large variations of k' (Huggins constant) values with time and temperature and low sedimentation velocities. The inserted PMMA made without crosslinking had dilute-solution properties similar to those of conventional bulk PMMA. In continuing the study, Blumstein[6] calculated the polydispersity parameter $\bar{M}_w/\bar{M}_n$ of the inserted polymer and found that it varied between 3 and 6 from gel permeation chromatography (GPC) data. The insertion polymer[7] was found to be much more isotactic than the bulk reference polymer. This type of tacticity was explained to be caused by the interaction of the carbonyl group of the ester with the positive exchangeable ions on the surface of the substrate.

The purpose of this investigation was to characterize the PMMA–kaolin clay composite system and the resulting homopolymers and inserted polymers.

EXPERIMENTAL

The preparation of materials and experimental procedures used in the radiation polymerization of MMA–kaolin clay composites has already been discussed.[8] X-Ray analysis of the clay was performed using a Siemens Crystalloflex IV, Type V-13 diffractometer.

Thermal analysis was accomplished using a Mettler Thermal Analyzer. An air atmosphere was used with a flow rate of 1 liter/hr of air, and a temperature rise of 10°/min to a temperature of 1000°C.

Particle-size distributions were made on dried, undried, and dried-irradiated kaolin clays using the United States Bureau of Mines Sharples Micromerograph. The clays were screened through a 200-mesh sieve, mixed with an antistatic agent (20% by volume Anstac M and 80% isopropyl alcohol), vacuum dried, placed in the injection port, and forced through a deagglomerator (set at 250 microns) using nitrogen pressure at a 100 lb/sq in. The distribution was calculated using the appplication of a corrected form of Stokes' law of fall for the velocity of particles falling in a gas. The surface area was determined with a three-point B.E.T.[9] determination using a Perkin-Elmer Model 212D Sorptometer.

Total Composite

Thermal gravimetry was performed as on the clay. Samples of total composite were investigated using the Jeolco JSM-2 scanning electron

microscope. All samples were fractured at room temperature and mounted on a copper disc using a silver conducting paste. A thin film of gold was vapor deposited under vacuum on the samples because they were nonconductors.

Mechanical tests were performed on bulk and 50:50 composite specimens using a Tinius Olsen compression tester. The middle range was used, which had a maximum compression of 12,000 lb. The sample specimens were cut and machined on a lathe and had the dimensions of 0.5 in. in diameter (compression area = 0.1963 sq in.) and 1.0 in. in length. An average compression rate of 1000 lb/min was applied, with the tests being performed at ambient temperature. The yield point for the composite was taken when the composite fractured and a maximum value was indicated on the gauge while still applying compression. The yield point for the bulk polymer was determined when the indicator hesitated while continuing to apply compression and then increased very swiftly to maximum compression on the gauge.

Homopolymer and Inserted Polymer

Thermal analysis was performed on selected samples of homopolymer using the same procedure as the clay analysis.

Relative molecular weight and molecular weight distributions of all polymers were obtained using a Waters Ana-prep gel permeation chromatograph (GPC). Styrogel was used as a column packing and toluene as solvent. The samples were filtered through a glass fiber syringe filter before injection into the GPC. Standard calibration curves of polystyrene were used for calibration of peak molecular weight.

All infrared spectra were obtained using a Beckman IR-12 spectrophotometer. The polymer was dissolved in dichloromethane, placed in an aluminum dish, and allowed to evaporate. The spectra were obtained from the film which remained.

Intrinsic viscosities and viscosity-average molecular weights of selected samples dissolved in benzene and toluene were determined using a Cannon-Ubbelohde semimicro dilution viscometer (Number 50) at 30° ± 0.02°C. The efflux times of solvent and solutions were greater than 100 sec; therefore kinetic effects were neglected.

NMR spectra were obtained using a Varian A-60 nuclear magnetic resonance spectrometer. The freeze-dried polymer was dissolved in *o*-dichlorobenzene. Due to the high molecular weights of the polymers and the subsequent high viscosities of the polymer solutions, only 5–7% solutions could be transferred to the NMR tubes. The solutions were frozen in NMR tubes using liquid nitrogen and sealed under vacuum. Spectra were obtained at approximately 150°C. Interpretation of the spectra was based upon statistical correlations reported by Reinmoller and Fox.[10,11]

RESULTS

Clay

X-ray. X-ray diffraction patterns of undried clay, dried clay, irradiated dried clay, and the insoluble composite after removal of homopolymer were obtained. The curves of all spectra taken appeared to be identical, and no shifting of peaks was observed. On the basis of the x-ray data it was assumed that there were no major disruptions in the structure of the clay lattice caused by either drying or irradiation. However, these data give no information concerning the number of changes in character of the active polymerization sites.

Particle Size and Surface Area. Particle-size distributions are shown in Table I. The distributions of undried, dried, and dried-irradiated clay indicated no breakdown in apparent particle size during irradiation. The micrographs obtained by scanning electron microscopy (SEM) show that the actual numbers obtained are not correct and that the sizes of clay agglomerates are being measured. The agglomerates are composed of many individual clay particles. The specific surface area of irradiated clay was found to be 16.64 sq meters as compared to 16 ± 1.0 sq meters found in the literature.[12]

TABLE I
Analysis of Particle Size Distribution for Various Treatments of Kaolin Clays

Clay system	% less than 10 μM diameter	% less than 4.6 μM diameter
Undried	85.6	50.0
Dried	79.9	50.0
Dried-irradiated	82.9	50.0

Thermal Analysis. Using DTA-TGA analysis, the kaolin clay was found to be stable through 400°C. However, in the range of 475° to 500°C, the clay underwent a normal transition due to the loss of hydroxyl groups from its lattice. This analysis was important in determining the amount of inserted polymer in the composite.

These analyses of the clay indicate that the irradiation by gamma rays had no effect on the overall structure, average particle size, and the average specific surface.

Polymer–Clay Composite

Thermal Analysis. Thermal analysis was performed on the total composite, inserted composite, homopolymer, and bulk polymer. As shown in Table II, the comparison of all systems in air for all polymerization temperatures shows that there was substantially no difference in the decomposition temperatures of the different irradiated polymers. These decomposi-

TABLE II
Decomposition Temperatures of Various Systems Using Air and Argon Atmospheres

Component	Polymer reaction temp., °C	Atmosphere	Heating rate, °C/min	Decomposition temp, °C
Total	50	air	10	310
composite	25	argon	6	330
Inserted	50	air	10	310
composite	25	air	10	305
	75	argon	10	320
	25	argon	6	320
Homopolymer	50	air	10	300
Bulk polymer	75	air	10	315
(irradiated)	50	air	10	310
	25	air	10	310
	25	argon	6	330
Bulk polymer (chemical)		air	10	280

tion temperatures fall in the range of 305°–315°. Decomposition beyond this temperature is rapid. The experiments using the argon atmosphere showed an increase in decomposition temperature of 10° to 20°C above the temperature in air due to the absence of the oxidizing atmosphere and difference in heating rate. The final decomposition temperature of all systems was 390–400°C at the same heating rate in air.

In comparing the irradiated systems with chemically initiated commercial PMMA, it was found that irradiation had increased the decomposition temperature 20°C above that of the commercial polymer (at the same experimental conditions).

Physical Appearance. The bulk polymer system when irradiated retained the clear, transparent properties of common Plexiglas. However, in some cases offgassing occurred in the polymer and gas bubbles were noted throughout the system.

The composite samples showed a variation in structure in the finished product. Some samples were solid throughout, but many samples had voids or pinholes. These voids could be caused by a number of things, such as improper filling of sample container or offgassing of the polymer. Offgassing was prevalent in these irradiation polymerizations.

Mechanical Properties. A comparison was made of the bulk polymers and composites at various reaction temperatures at a dose rate of 12.9 rads/sec. The total doses obtained were approximately 100,000 (25°C), 70,000 (50°C), and 60,000 (75°C) rads past the system endpoints. The doses were reduced as the temperature increased because of depolymerization effects on the samples; however, the dosage was necessary to ensure that the samples were polymerized fully. No unreacted monomer was evident in any of the systems. These doses are not to be construed as

TABLE III
Compressive Strength Data

Polymer	Compressive strength, psi × 10^{-3}	Sample size
Bulk—irradiated	16.4 ± 0.6	10
50:50 Composite—irradiated	18.3 ± 0.4	22
50:50 Composite—chemical	17.3 ± 0.5[40]	11
Bulk—chemical[43]	11–16	
Epoxy—various fillers	15–25	
Furane—asbestos filler	10–13	
Melamine—formaldehyde—cellulose filler	25–45	
Phenol—formaldehyde—glass fiber	17–70	
Phenolic—mineral filler	29–34	
Polyester—chopped glass	15–30	
Silicones—glass fiber	10–15	
Urea—formaldehyde—cellulose filler	25–45	

optimum doses and were just used to see if gross differences existed in the mechanical properties of the polymers.

Results of the compression tests are shown in Table III, along with composite compressive strengths for other polymer system. The following comments can be made: (1) The compressive strengths of all samples polymerized at 25°, 50°, and 75°C were the same, within experimental error. (2) Within the time limits of these experiments, the compressive strengths were the same for different total doses beyond the endpoint.

The results reported in Table III represent average values of samples prepared under different conditions of temperature and total dose. The addition of the clay to the polymer system did not result in a decrease in compressive strength. A small increase in strength was actually noted. In most polymer systems, the addition of anything except fibrous fillers results in a decrease of mechanical properties. Therefore, it is clear that the addition of the clay had a beneficial effect on this system and that further improvements could possibly be obtained through the use of fibrous materials, particularly the addition of kaolin fibers.

Scanning Electron Microscopy. Throughout this study composite samples were examined by SEM. It was concluded that SEM did not reveal any major differences in any of the samples regardless of the dose rate, total dose, or temperature employed. Several general features were noted and are described in the following paragraphs.

Figure 1 shows a typical composite fracture surface. These micrographs revealed numerous bulk agglomerates (20–100 μ) surrounded by a more uniform matrix. Higher-magnification micrographs showed that the large agglomerates were made up of smaller agglomerates (2–6 μ). A sufficient number of micrographs were recorded to conclude that the clay

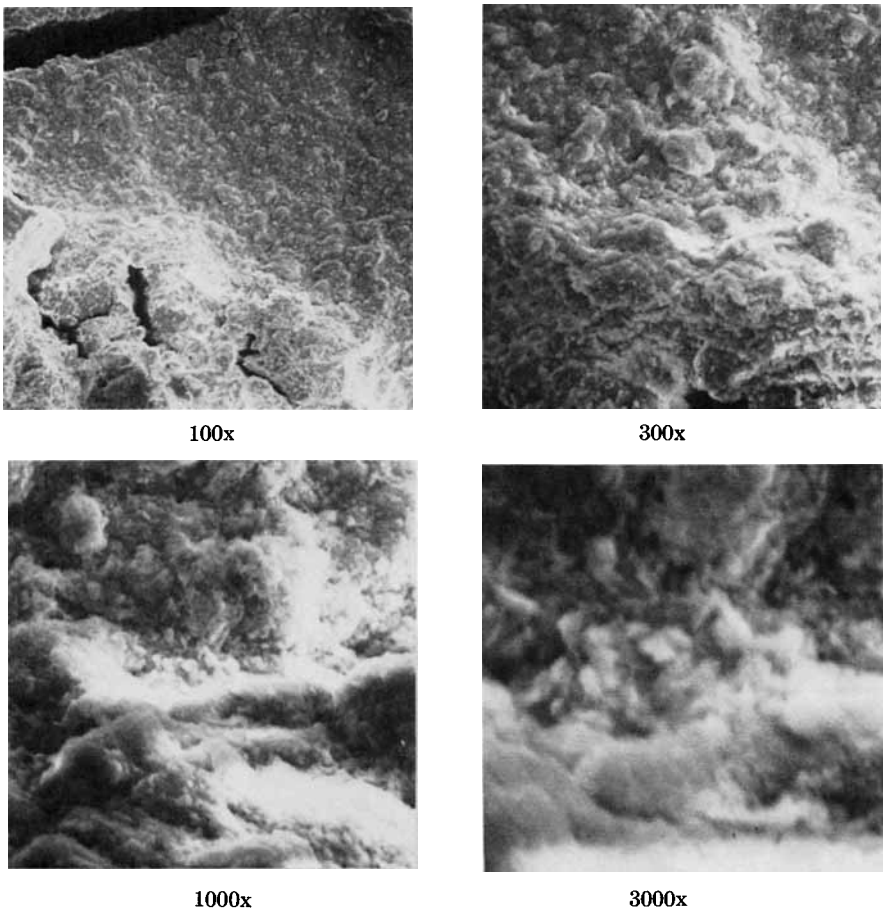

Fig. 1. Micrograph of total composite: 1μ = 0.04 in. for 1000 ×; 1μ = 0.133 in. for 3000 X

agglomerates were wetted. A number of different mixing procedures were tested (including high-shear blending, high-frequency mechanical vibrating, and ultrasonic waves) in an attempt to better disperse the clay. None of the approaches was successful. The size of the individual clay particles were beyond the resolution limits of the SEM. It was therefore concluded that the particle size analysis reported reflects only the dimensions of the clay agglomerates in air.

Figures 2 and 3 are representative of the inserted polymer–clay surfaces after the homopolymer had been dissolved. These micrographs show a surface composed of agglomerates (>20 μ) which have been smoothed through the dissolution process. No surface detail is evident, since the entire surface is covered with a thin layer of polymer which has been smoothed by the solvent extraction process.

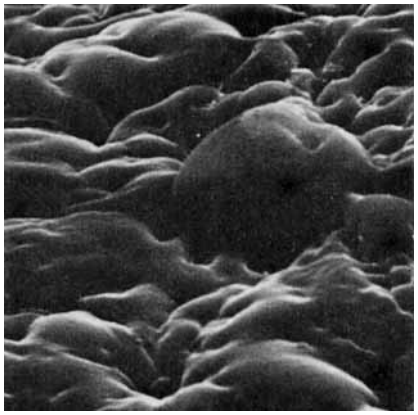

300x

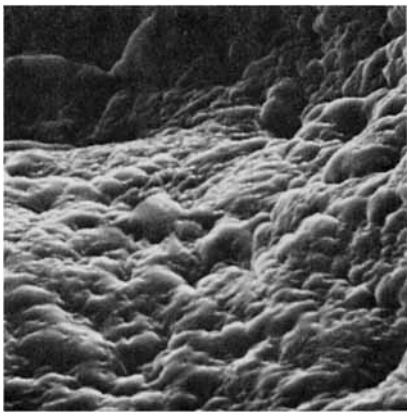

1000x

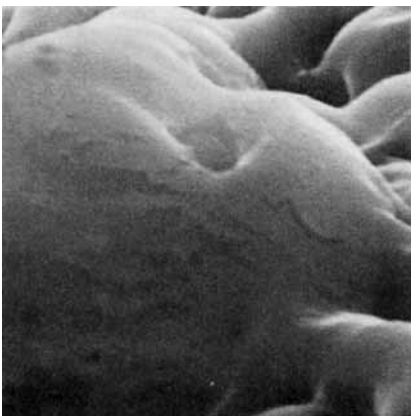

3000x

Fig. 2. Micrograph of insoluble composite: distance as in Fig. 1.

Figure 4 shows the inserted clay–polymer surface after digestion with hydrofluoric acid. The residue remaining shows the clay agglomerates in more detail. The smooth portions of the surface are bits of polymer–clay which were apparently unaffected by the acid treatment.

Homopolymer and Inserted PMMA

Infrared Spectroscopy. Infrared spectroscopy was used to determine whether or not any gross changes occurred in the structure of the PMMA caused by irradiation or if there was a difference in the structure of the homopolymer and inserted composite of the polymer. No differences in the spectra of the inserted polymer and homopolymer were noticed for any of the various irradiation times, reaction temperatures, and dose rates.

Intrinsic Viscosity and $\bar{M}_v$. In the formation of polymer in the bulk system, initial polymer chains formed which then migrated through the re-

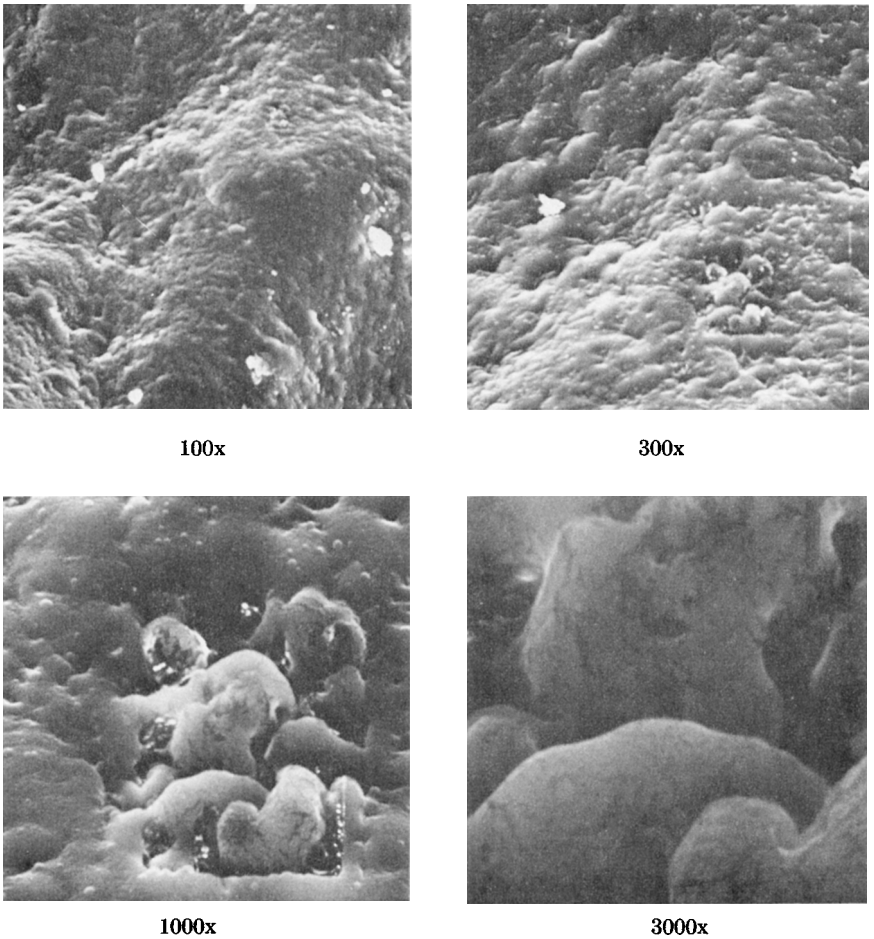

Fig. 3. Micrograph of insoluble composite: distance as in Fig. 1.

action media (largely monomer). In some cases these chains were shown to actually settle to the bottom of the reaction mixture. A diffusion-controlled mechanism therefore probably started at a lower percentage conversion.

Chemically initiated systems have no tendency toward chain breakdown during polymerization. Two opposing reactions occurred when gamma irradiation was used. The polymerization reaction was actually a net process of polymerization and depolymerization. After the polymer became a gel, further irradiation increased the depolymerization reaction and decreased the molecular weight of the reaction. The ultimate molecular weight of polymers formed via gamma initiation would therefore be expected to be less than for the chemically initiated commercial system. However, the molecular weights of the composite polymers formed in this

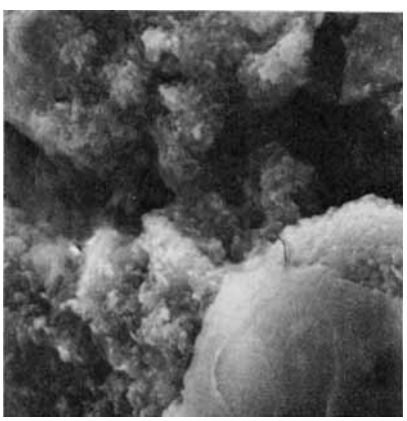

300x

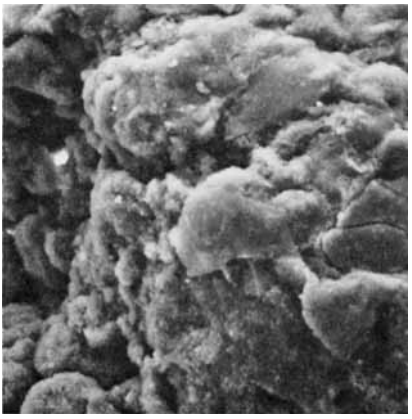

1000x

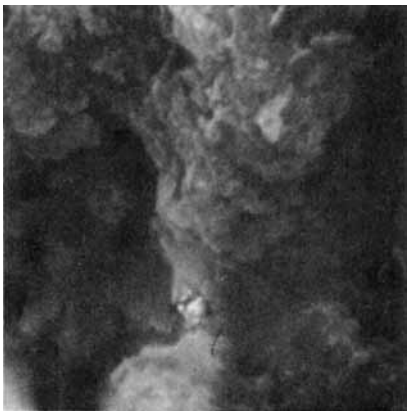

3000x

Fig. 4. Micrograph of HF-treated composite: distance as in Fig. 1.

study were somewhat higher than those polymers produced in the bulk by normal laboratory synthesis techniques and existing commercial processes.

Intrinsic viscosities reported in Tables IV and V were determined on the homopolymers and bulk polymers at their endpoints and at various times before their endpoints. Because of the high molecular weights of the polymers, special handling precautions were followed. Some of the polymers required dissolution times in excess of one week at ambient temperature. Molecular weights calculated from intrinsic viscosities in these two solvents agree within 5% of each other. The dissolution process could not be hastened by heating (to more than 40°–50°C) for fear of degrading the polymer.[13] Solutions could not be agitated beyond a gentle stirring because of possible degradation of the polymers by localized shear stresses.[14,15] The dissolution was therefore allowed to occur with a minimum of heating and stirring.

TABLE IV
Intrinsic Viscosity Data at Endpoints for Homopolymers and Bulk Polymers

Trial	$[\eta]$	k'	k''	$k' + k''$	$\bar{M}_v \times 10^{-6}$	Temp., °C	Atm.	Solvent[a]	Dose rate, rads/sec	Total dose, rads $\times 10^{-3}$
68-3D-A	4.17	.242	.226	.468	2.84	25	air	B	7.35	225
68-5B-B-C	3.50	.338	.160	.498	2.26	25	air	B	12.9	313
68-5-C	3.42	.447	.070	.517	2.19	25	air	B	24.9	457
74-3D-B	5.80	.414	.113	.527	4.38	50	air	B	7.35	140
74-3B-C	4.55	.406	.097	.503	3.18	50	air	B	12.9	183
74-7-A	4.21	.274	.210	.484	2.87	50	air	B	24.9	264
73-1D-B	5.94	.312	.174	.486	4.52	75	air	B	7.35	90
73-5-B-D	6.71	.198	.279	.477	5.30	75	air	B	12.9	120
69-5B-C	4.45	.307	.180	.487	3.09	25	argon	B	12.9	311
75-3B-A	4.89	.388	.116	.504	3.50	50	argon	B	12.9	180
68-5B-B-0	3.50	.338	.160	.498	2.26	25	air	B	12.9	313
68-5B-B-24	4.38	.292	.198	.490	3.03	25	air	B	12.9	313
68-5B-B-72	4.51	.311	.171	.482	3.14	25	air	B	12.9	313
74-3-B-D[b]	6.30	.258	.235	.493	4.88	50	air	B	12.9	210
73-5B-C[b]	6.28	.340	.153	.495	4.86	75	air	B	12.9	130

[a] B = Benzene.
[b] Bulk polymer

TABLE V
Intrinsic Viscosity Data Approaching Endpoints for Homopolymers and Bulk Polymers

Trial	$[\eta]$	k'	k''	$k' + k''$	$\bar{M}_v \times 10^{-6}$	Temp., °C	Atm.	Solvent[a]	Dose rate, rads/sec	Total dose, rads $\times 10^{-3}$
66-5D-F	.16	.345	.151	.496	.88	25	air	T	7.35	72
66-4D-F	1.10	.375	.137	.512	.81	25	air	T	7.35	109
66-2D-F	1.17	.370	.140	.510	.88	25	air	T	7.35	146
68-3D-A[b]	4.17	.242	.226	.468	2.84	25	air	B	7.35	225
66-5B-E	.90	.407	.115	.522	.61	25	air	T	12.9	99
66-4B-E	.91	.390	.132	.522	.62	25	air	T	12.9	152
66-2B-E	.98	.382	.135	.517	.69	25	air	T	12.9	208
68-5B-B-0[b]	3.50	.338	.160	.498	2.26	25	air	B	12.9	313
66-2-I	.76	.340	.156	.496	.48	25	air	T	24.9	147
66-6-4-D-I	.77	.372	.136	.508	.49	25	air	T	24.9	230
68-5-C[b]	3.42	.447	.070	.517	2.19	25	air	B	24.9	457
66-2-A-I[c]	.72	.281	.192	.473	.45	25	air	T	24.9	194
66-3-A-I[c]	.68	.284	.202	.486	.41	25	air	T	24.9	402
66-4-A-I[c]	.83	.339	.158	.497	.55	25	air	T	24.9	512
70-RT-7 Days	8.50	.341	.154	.495	7.29	25	air	B	0	0

[a] B = benzene; T = toluene.
[b] At endpoint.
[c] Bulk polymer.

The molecular weights were calculated using literature values for the constants in the Mark-Houwink equations:

$$[\eta] = KM_v^a$$

For benzene[16]: $K = 5.2\times10^{-5}$ $a = 0.76$
For toluene[17]: $K = 7.0\times10^{-5}$ $a = 0.71$

The following general trends were drawn from the endpoint data shown in Table IV:

1. The net viscosity-average molecular weight ($\bar{M}_v$) of composite polymers produced at a constant temperature increased as the dose rate decreased.
2. At a constant dose rate, the $\bar{M}_v$ of the composite polymers increased as temperature increased (from 25° to 75°C).
3. The molecular weights of the homopolymers formed in the presence of an inert gas (argon) were slightly higher than those of homopolymers produced in air at similar temperatures and dose rates.
4. Trials 68-5B-B-0, 68-5B-B-24 and 68-5B-B-72 represent a composite polymer that was polymerized in air at 25°C using a dose rate of 12.9 rads/sec, but where dissolution was started immediately after the endpoint (-B -0), after 24 hr (-B -24), and after 72 hr (-B -72). Published data indicated that polymerization could continue after irradiation if a sufficient amount of unconverted monomer remained. The molecular weight data indicate that the monomer reacted with the existing growing chain ends in the absence of radiation and formed higher molecular weight polymers.
5. The $\bar{M}_v$ of both irradiated composite and bulk polymers was higher than the same system formed by the use of a chemical initiator (5×10^5).[18]

The following trends can be stated for the bulk and homopolymers which approach the endpoint at various experimental conditions (Table V):

1. At a constant temperature and dose rate, only slight increases in $\bar{M}_v$ of the polymer were in evidence until the endpoint was reached. The tremendous increase in $\bar{M}_v$ at the endpoint showed the importance of the Trommsdorff effect.
2. At a constant temperature, the $\bar{M}_v$ of the polymer was higher as dose rate decreased.
3. Trial 70-RT-7 was obtained for a sample which was polymerized at ambient temperature in air for seven days in the complete absence of any irradiation. The resulting polymer had a higher molecular weight than any of the polymers formed in the presence of radiation ($\bar{M}_v = 7.2\times10^6$). In this instance, depolymerization and degradation reactions would not be expected to occur.

The intrinsic viscosity data of the inserted polymer at the endpoints is shown in Table VI. The molecular weights, intrinsic viscosities were of the same magnitude as the homopolymer. The comparison of the inserted polymer formed in these studies with those of Blumstein[3] indicate that much larger molecular weights were obtained for the inserted polymer

TABLE VI
Intrinsic Viscosity Data at Endpoints for Inserted Polymers

Trial	$[\eta]$	k'	k''	$k' + k''$	$\bar{M}_v \times 10^{-6}$	Temp., °C	Atm.	Solvent[a]	Dose rate, rads/sec	Total dose, rads $\times 10^{-3}$
68-3D-A	2.56	.342	.142	.484	2.70	25	air	T	7.35	225
68-5B-B	3.32	.393	.127	.520	3.86	25	air	T	12.9	313
68-5-C	2.22	.362	.138	.500	2.18	25	air	T	24.9	457
74-3D-B	2.00	.410	.123	.533	1.89	50	air	T	7.35	140
74-7-A	2.33	.430	.119	.549	2.34	50	air	T	24.9	264
73-1D-B	1.96	.403	.114	.514	1.83	75	air	T	7.35	90

[a] T = toluene.

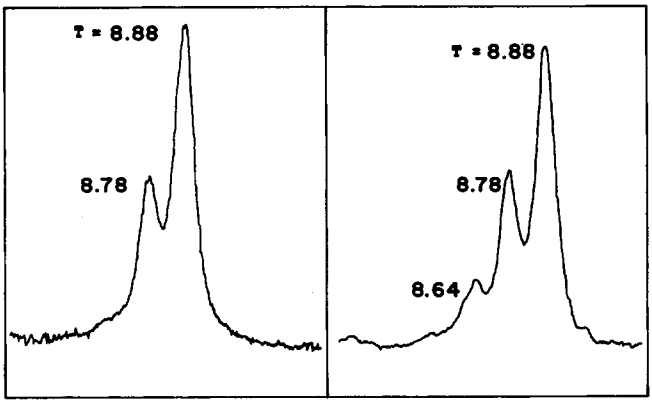

Fig. 5. NMR spectrum of bulk and inserted polymers.

in the kaolin clay complex than with the sodium montmorillonite and other types of inorganic substrates.[1] This difference will be discussed further in comparing the NMR results.

The values of k' and k'' reflect the extent of polymer–solvent interactions. These values as shown in the table do not have a direct relationship to the molecular weight. However, as the $\bar{M}_v$ increased, most of the k' values increased above the normal 0.30 to 0.35 for the solvents used, showing that the polymer was becoming more difficult to place into solution. The values of k' could also reflect the changes in the molecular weight distribution and tacticity.

GPC. Selected samples of both types of polymer were subjected to GPC analysis. Molecular weights and molecular weight distribution relative to each other were found to be the same. A sample distribution peak was obtained for the endpoints of both types of polymer at a peak molecular weight of greater than 5×10^6 when compared to the polystyrene calibration curve.

Nuclear Magnetic Resonance. NMR spectra were obtained on selected samples of the bulk polymer, homopolymer, and inserted polymer. Figure 5 shows the pertinent portions of spectra for a bulk polymer and an inserted polymer.

In interpreting the spectra for PMMA, consideration must be given to the influence of both the adjacent and nearest neighboring α-methyl groups on the methylene protons. The signals generated reflect the stereospecificity of the polymer chain. The optical configuration of two adjacent monomer units which are the same are classified as isotactic (I) placements. Those having different configurations are classified as syndiotactic (S) placements. When three adjacent monomer units are considered, either isotactic pairs of placements (II), syndiotactic pairs (SS), or heterotactic pairs (IS_vSI) can be formed.

TABLE VII
Average Tacticities of PMMA–Kaolin Polymers in *o*-Dichlorobenzene at 150°C

System	No. of trials	P(SS)	P(ISSI)	P(II)	P(IS)	P(S)	P(I)
Bulk polymer	9	.63	.32	.05	.16	.79 ± .02	.21 ± .02
Homo-polymer	23	.58	.34	.08	.17	.75 ± .02	.25 ± .02
Inserted polymer	7	.54	.34	.11	.17	.72 ± .03	.28 ± .03

The data reported are based upon placement pairs. As seen in the figure, the signals at 8.64, 8.78, and 8.88τ represent the pairs of placements II (isotactic), IS,SI (heterotactic), and SS (syndiotactic), respectively. The values calculated are in agreement with those values reported by Reinmoller and Fox at 8.62, 8.75, and 8.85 for the same pairs of placements.[10]

Table VII gives data and results for a series of polymers formed under different conditions. The data presented in the table show that the bulk polymer is highly syndiotactic and lies in the normal range expected for a free-radical polymerization. This tacticity is consistent with the interpretation of the kinetic data. Spectrum 68-5B-B is typical for the homopolymers and inserted polymers. In all cases a change in the stereospecificity has occurred. The table shows that the isotacticity has increased in both the homopolymers and inserted polymers. While these changes are statistically significant, the polymers are still largely syndiotactic, indicating that a free-radical mechanism prevails.

The changes in tacticity are relevant when the data are compared to those reported by Blumstein et al.[7]. The ratio of MMA to montmorillonite used by these authors assumed to constitute a monolayer. The tacticity of the polymers formed was largely isotactic where P(I) was about 0.59. They concluded that the mechanism which leads to the isotactic stereospecificity was confined to the surface of the mineral and P(II) and P(SS) were not temperature dependent. The sodium montmorillonite surfaces possessed exchangeable cation sites which were distributed on the negatively charged lamellae and could associate with the MMA through the carbonyl pendant ester group. The population of exchangeable ions was sufficient to coordinate large numbers of MMA molecules by dipole–ion interactions. Monomers which were coordinated in this manner would be expected to have limited mobility. However, the molecules could exhibit greater degrees of freedom depending upon the orientation of the surrounding molecules. Those monomer molecules which were associated on the lamellae surface and which were in the correct orientation could only form isotactic placements. The growing chain would then be determined by the proportions of associated to unassociated monomer units. It was assumed that the interaction between the lamellae surface and the non-

associated monomer was insignificant and that the monomer would behave as if polymerized in the bulk.

In the 50:50 weight ratios reported here, there was always a preponderance of unassociated monomer molecules. Therefore, the fraction of monomer which could associate is small. If the above mechanism were completely valid for the present system, one would expect that the homopolymer (that dissolved from the composite) would have the same tacticity as polymer formed in the bulk polymerization. The data presented in Table VII indicate that both the homopolymer and the inserted polymer have increased isotacticity. The kaolin clay used in the present study had fewer (unsaturated) cations concentrated on the crystal edges than sodium montmorillonite (concentrated on the lamellae surface). This fact would account for the lower tacticity of the inserted polymer on the kaolin clay than on the montmorillonite complex.

The above mechanism does not account for changes in tacticity of the homopolymer of the composite reported here. A possible explanation to account for the homopolymer tacticity is to consider the possibility of polymer–monomer exchange on the clay surface.[19] It is postulated that the initial monomer on the clay surface can be held by dipole-ion, hydrogen bonding, or dipole–dipole interactions. A series of (II) placements result in an initial polymer chain having increased isotacticity. As the chain grows in length and establishes its stereo helix, the strain exerted in sections of the chain by a particular conformation of the polymer can overcome the surface interaction and break the growing polymer away from the surface. Energy could also be absorbed by the polymer chain from the radiation. If this would happen, then segments of the chain could reach an excited state or absorb enough energy to break away from the clay surface after being orientated on the surface. If these reactions would occur, a mobile monomer unit could immediately diffuse to the surface and the orientation–excitation process would be repeated until the gel point was reached. From this point, the polymerization process would be diffusion controlled and no further exchange would take place. The result would be that both the homopolymer and the inserted polymer would have essentially the same tacticity, but would have the following order of tacticity of polymer: inserted > homo > bulk.

CONCLUSIONS

The kaolin clay substrate had no apparent structural changes due to the irradiation process. The composite formed by irradiation was mechanically as stable under compression as bulk polymer and had a higher degradation temperature.

The characterization of the homopolymer and the inserted polymer indicates that high molecular ($1–5 \times 10^6$) weights are formed for both types of polymer. The molecular weights of the homopolymer and bulk polymer increased as temperature and dose rate decreased. The tacticities of the homopolymer and the inserted polymer were greater than that of the bulk-

irradiated polymer at all temperatures and dose rates. The homopolymer tacticity was intermediate between that of the inserted polymer and that the bulk polymer, indicating that the clay substrate had some effect on the polymer surrounding it.

The authors wish to thank the Atomic Energy Commission (Grant No. AT(11-1) 2057) for their support of this work.

References

1. B. L. Tsetlin, S. R. Rafikov, L. I. Plotnikova, and P. Ya. Glazunov, *Proceedings of the Second All-Union Conference on Radiation Chemistry, Moscow, Oct. 10–14, 1960,* 529 (1964).

2. T. P. Kornienko, U. N. Polishchuk, T. G. Zelenchukoca, and M. V. Polyakov, *Proceedings of Radiation Chemical Materials Symposium of Polymers Moscow,* 1964, 69 (1966).

3. A. Blumstein, *J. Polym. Sci. A,* **3,** 2653 (1965).

4. A. Blumstein, *J. Polym. Sci. A,* **3,** 2665 (1965).

5. A. Blumstein and F. W. Billmeyer, Jr., *J. Polym. Sci. A-2,* **4,** 465 (1966).

6. A. Blumstein, R. Blumstein, and T. H. Vanderspurt, *J. Colloid Interface-Sci.,* **31**(2), 236

7. A. Blumstein, S. L. Malhotra, and A. C. Watterson, *J. Polym. Sci. A-2,* **8,** 1599 (1970).

8. J. J. Beeson and K. G. Mayhan, *J. Appl. Polym. Sci.,* **16,** 2765 (1972).

9. J. Currier, International Minerals and Chemical Corporation, Libertyville, Illinois, personal communication.

10. M. Reinmoller and T. G. Fox, *ACS Polymer Preprints,* **17**(2), 987 (1966).

11. M. Reinmoller and T. G. Fox, *ACS Polymer Preprints,* **17**(2), 999 (1966).

12. R. E. Grim, *Clay Mineralogy,* McGraw-Hill, New York, 1968, p. 265.

13. Y. C. Chen, M. S. Thesis, University of Missouri-Rolla, 1965.

14. T. F. Niu, M. S. Thesis, University of Missouri-Rolla, 1970.

15. A. A. Sarmasti, M. S. Thesis, University of Missouri-Rolla, 1970.

16. J. Brandrup and E. H. Immergut, Eds., *Polymer Handbook,* Interscience, New York, 1966, p. IV–26.

17. *Ibid.,* p. IV–28.

18. K. G. Mayhan and L. F. Thompson, GCMR, University of Missouri-Rolla, personal communication.

19. G. Bertrand, University of Missouri-Rolla, personal communication.

Received April 24, 1972